Available online at www.sciencedirect.com

SCIENCE DIRECT

ELSEVIER

Tectonophysics 418 (2006) 219–234

TECTONOPHYSICS

www.elsevier.com/locate/tecto

Short-term vertical velocity field in the Apennines (Italy) revealed by geodetic levelling data

E. D'Anastasio [a,b,*], P.M. De Martini [a,c,1], G. Selvaggi [a,b,1], D. Pantosti [a,1], A. Marchioni [d,2], R. Maseroli [d,2]

[a] *Istituto Nazionale di Geofisica e Vulcanologia, via di Vigna Murata 605, 00143, Roma, Italy*
[b] *Istituto Nazionale di Geofisica e Vulcanologia, Centro per la Sismologia e l'Ingegneria Sismica, via Castello d'Aquino 13, 83035, Grottaminarda (AV), Italy*
[c] *UMR 7516, IPG Strasbourg, EOST, Universite' Louis Pasteur, Strasbourg, France*
[d] *Istituto Geografico Militare, Servizio Geodetico, via di Novoli 93, 50127, Firenze, Italy*

Received 21 July 2005; received in revised form 10 February 2006; accepted 14 February 2006
Available online 17 April 2006

Abstract

We estimate current vertical movements along the Apennines (Italy) through repeatedly measured high precision levelling routes. In order to highlight regional crustal deformation the analysis of a geodetic database, with a minimum benchmark density of 0.7 bm/km (1943–2003 time period), is carried out. We evaluate systematic and random error and their propagation along the levelling routes. Tests on original raw height data have been carried out to define error propagation. The computed relative vertical rates stand significantly above error propagation. A series of traverses along and across the Apennines and a map of relative vertical velocities reveal a geodetic signal characterised by values up to 2.5–3.0 mm/a and by wavelengths up to 100 km.

Keywords: Geodesy; Comparative levelling; Elevation changes; Apennines; Neotectonics

1. Introduction

It is widely reported that regional uplift is a first order dynamic driving mechanism of the main peninsular mountain range of Italy: the Apennines (see, e.g.: Cinque et al., 1993; Bordoni and Valensise, 1998; Amato and Cinque, 1999; D'Agostino et al., 2001; Patacca and Scandone, 2001; Bartolini, 2003; among many others). A widespread surface uplift occurred during the last 1 million years is shown by many geological and geomorphological data, indicating an average uplift rate of about 1 mm/a (e.g.: Bordoni and Valensise, 1998; D'Agostino et al., 2001, and references therein). Current deformation of the Apennines is due to a complex geodynamic setting. From a simple kinematic point of view, the NW–SE trending range of northern and central Apennines (inset of Fig. 1) is characterised by NE–SW active lengthening, while eastward, toward the

* Corresponding author. Istituto Nazionale di Geofisica e Vulcanologia, CNT, via di Vigna Murata 605, 00143, Roma, Italy. Tel.: +39 06 51860564; fax: +39 06 51860507.
E-mail addresses: danastasio@ingv.it (E. D'Anastasio), demartini@ingv.it (P.M. De Martini), selvaggi@ingv.it (G. Selvaggi), pantosti@ingv.it (D. Pantosti).
[1] Fax: +39 06 51860507.
[2] Fax: +39 055 417909.

0040-1951/$ - see front matter © 2006 Elsevier B.V. All rights reserved.
doi:10.1016/j.tecto.2006.02.008

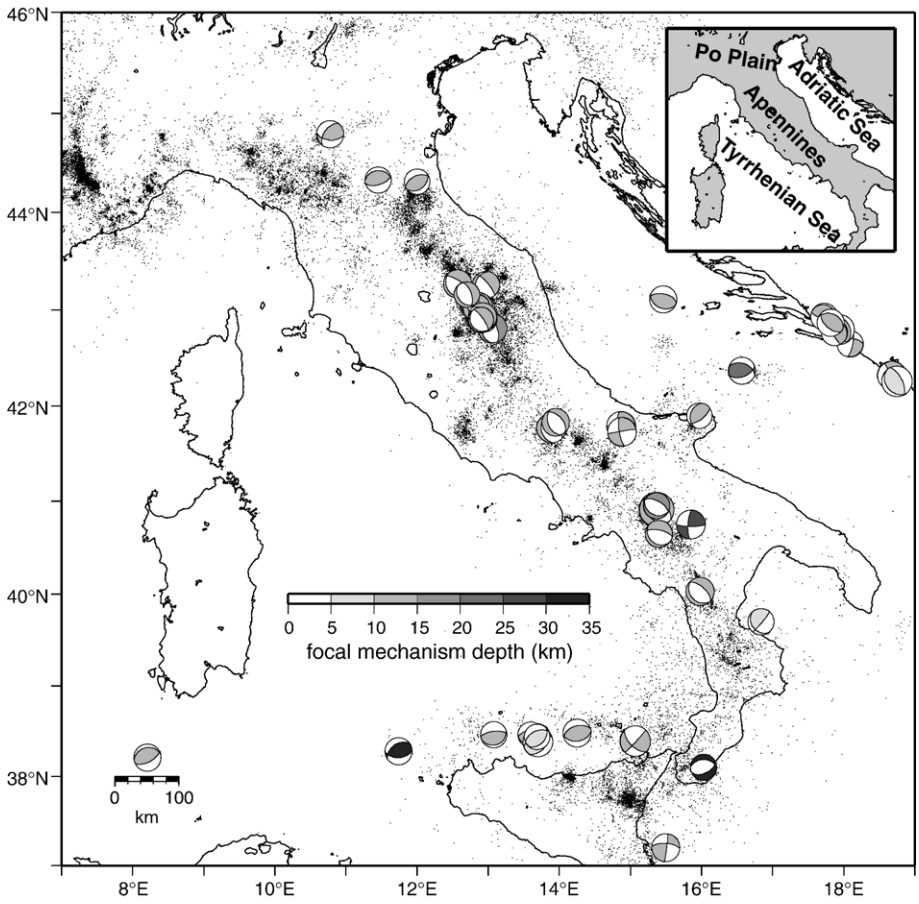

Fig. 1. Map of the Italian seismicity. Instrumental seismicity (1983–2004) (after Castello et al., 2004; Chiarabba et al., 2005), and CMT (Harvard, http://www.seismology.harvard.edu/projects/CMT/) and RCMT (Pondrelli et al., 2002, 2004; http://www.ingv.it/seismoglo/RCMT/) focal plane solutions of earthquakes with M_W greater than 5.0 and depth lower than 35 km are shown; focal mechanism depths are shown with the grey scale.

Adriatic Sea, focal plane solutions of crustal earthquakes indicate NE–SW shortening (e.g.: Pondrelli et al., 2002, among many others) (Fig. 1). The southern Apennines are characterised by NE–SW oriented active extension within the range, and by a lack of evidence of shortening in its outer part, as clearly indicated by recent GPS solutions (D'Agostino and Selvaggi, 2004; Serpelloni et al., 2005). Horizontal rates of shortening and lengthening are at the level of a few mm/a (Hunstad et al., 2003; D'Agostino and Selvaggi, 2004; Serpelloni et al., 2005).

On the other hand, estimates of vertical motion are mainly derived from geological or geomorphological data, and present day geodetic estimates are still lacking. In this work we approach the problem of estimating vertical motion in the Apennines using a network of first order levelling lines that sample the peninsula from the Adriatic towards the Tyrrhenian Sea, crossing the Apennines. The aim of this paper is to provide a quantitative description of the short-term vertical velocity field across the Apenninic chain. We use levelling data because three main advantages pertain to them compared to GPS data: (a) the resolution in evaluating the vertical component of motion is one order of magnitude better than GPS to GPS estimates; (b) no comparable sampling of active regions (<1 benchmark per km) is presently available from GPS networks in Italy; (c) it is the only geodetic dataset regarding vertical movements that spans back in time to the past 50–100 years. On the contrary, the main disadvantage of levelling measurements is the lack of an absolute reference datum, and only relative motion can be precisely determined by comparative levelling data (Bomford, 1971).

The only previous general study on geodetic levelling estimates of current vertical movements in Italy has been conducted by Arca and Beretta (1985). These Authors readjusted levelling data, measured in northern Italy during two major campaigns (1877–1903 and 1950–1956), applying a correction for sea level variations occurred between the first and second surveys, and a

correction for the time difference between the effective survey years of each sector of the network and the 1897 and 1957 reference years (Salvioni, 1953, 1957). The resulting elevation changes show two main features: (a) an uplifting area, in the NW sector of northern Italy, with values up to 3.5 mm/a; (b) a subsiding area in the SE sector of northern Italy, with values up to 7 mm/a in the Po Plain (Arca and Beretta, 1985). After 1957, the Italian first order levelling network has been developed and enlarged, and new measures are now available. In order to better determine the current vertical velocity field of the whole Apennines we collected, georeferenced and analysed previously unpublished high precision levelling data, focusing our study on movements occurred during the past 50 years. In the following, after the description of the collected database, we present two complementary results: (i) a series of transects across and along northern and central-southern Apennines and (ii) a map of rates of vertical movements.

2. Levelling database

For over 120 years the Istituto Geografico Militare (IGM) has repeatedly measured the elevation of selected routes along the Italian peninsula (Fig. 2). The IGM first order (or high precision) levelling network has been measured since 1870 with high precision levelling techniques, following the International Geodetic Association standards defined in Oslo in 1948 (Vignal, 1936; 1950). The IGM high precision levelling standards, since 1940, require: (a) double levelling between consecutive benchmarks (maximum allowed discrepancy between forward and backward levelling of $\pm 2.5\ \sqrt{L}$ mm, where L is the length of the levelled segment, in km); (b) equal number of setup for forward and backward measurements; (c) circuits closure (maximum admitted misclosure of $\pm 2.0\ \sqrt{L}$ mm, where L is the circuit length, in km); (d) instrument calibration before and after each survey; (e) maximum allowed sight length of 50 m; (f) independent

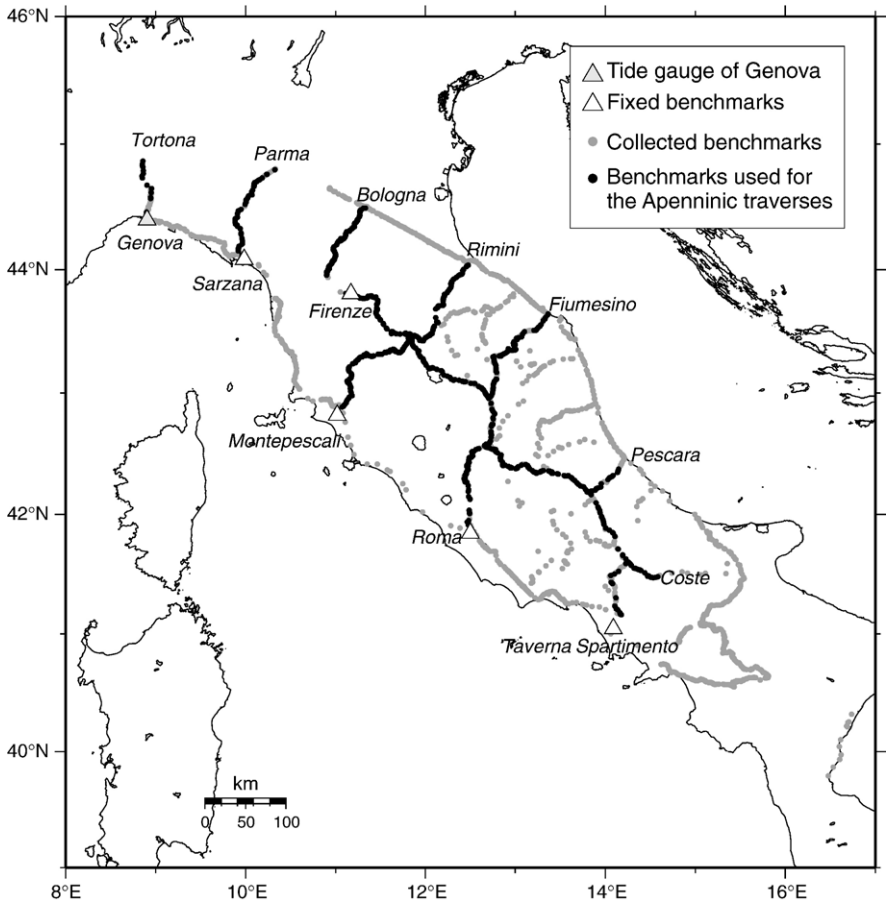

Fig. 2. Map of all the collected benchmarks measured at least two times from 1870 to 2003 (grey dots). Benchmarks measured two times in 1950 and 2000 along the Apenninic chain are also shown (black dots). White and grey triangles indicate, respectively, fixed benchmarks of each transect (see Figs. 6, 8 and 9) and the reference tide gauge of peninsular network.

measurements between consecutive line sectors ("fragmented" levelling every 15 km of line); (g) use of invar rod and rod correction (Salvioni, 1951; Muller, 1986).

The IGM first order network is composed by 14,000 km of levelling lines, and is presently under expansion. Consecutive benchmarks have an average distance of ca. 1 km, and are usually placed in groups of three each 5 km. The reference benchmark of the national network is the tide gauge of Genova (Fig. 2).

Courtesy of IGM, we collected adjusted heights of 65 levelling lines, for a total length of 5100 km and 3740 benchmarks of the first order levelling network, that were measured at least twice between 1870 and 2003 (Fig. 2). The IGM measured the whole levelling network during 1879–1905, 1943–1959 and 1980–2003. In the following, we refer to each of these sets of data as the "1890," "1950" and "2000" levelling measurements, respectively. Because of the large number of repeatedly measured benchmarks (more than 0.7 bm/km) and the higher precision compared to the 1890–1950 ones (less than 0.1 bm/km), we focused our investigation on the 1950 and 2000 levelling measurements. The first order levelling dataset we analysed in detail consists of 1325 benchmarks distributed over a total length of 1613 km (Fig. 2).

The standard error of the entire network, computed from loop misclosures and calculated by IGM for the 1950 network only, is ±0.72 mm/km (Salvioni, 1957). Since the levelling procedures remained nearly unchanged from 1950 until now, the IGM did not calculate the standard error of the "2000" network, and assumes that the 1950 and 2000 values are identical (Muller, 1986). Taking into account the precision of the 1950–2000 datasets, vertical velocities along the Apennines of the order of 1.0 mm/a, or more, are likely out of these standard errors.

3. Methods

3.1. Elevation change determination

We determine current vertical movements along the Apennines using adjusted height data (i.e., raw height data adjusted for circuit misclosure). Because of the lack of an absolute reference datum, we conduct the analyses in terms of relative elevation changes. In order to examine the vertical velocity field along the Apennines, we link consecutive levelling lines across the chain to construct a series of traverses from the Tyrrhenian to the Adriatic side of the peninsula. Relative elevation changes are referred to the westernmost benchmark of each traverse (Tyrrhenian side) (Fig. 2). This decision is taken because, according to Bordoni and Valensise (1998), most of the Tyrrhenian side of the Apennines has been essentially stable in the past 125 ka, with the exceptions of the Latium coast and the Campana Plain. A 0.2–0.4 mm/a uplift and subsidence was estimated in the Latium coast and the Campana Plain, respectively, during Upper Pleistocene. Thus the nodal benchmarks of Rome and Taverna S., located in these two areas, may behave accordingly (see Fig. 2). In most of the cases we select nodal benchmarks as the arbitrary fixed point of each transect, because of the higher number of checks and surveys that IGM usually makes on them. We then calculate relative vertical rates from relative elevation changes, using the time elapsed between repeated surveys of each line or line sector.

In order to check benchmark instability due to sediment compaction or groundwater changes, we define the lithology below each benchmark, based on geological maps at a scale 1 : 100,000 (see legends of Figs. 6–9). We thus proceed with removal of outliers, defined as those benchmarks clearly showing anomalous elevation changes with respect to adjacent line sectors. We remove from the profiles single benchmarks showing a positive or negative elevation change difference greater than an average value of 23 cm with respect to neighbouring benchmarks (minimum and maximum threshold values are, respectively, of 10 and 150 cm). Line sectors where the elevation change pattern clearly reflects non-tectonic signals (mainly related to groundwater withdrawal) have been removed too; vice versa tectonic signals for which a coseismic or volcanic origin could be easily identified, are left unmodified but excluded from further analysis and interpretations.

3.2. Error estimation

Systematic and random errors, and their propagation, affect levelling lines (e.g.: Bomford, 1971). When levelling data are used for tectonic purposes (i.e., as in our case, to study regional vertical movements), it is important to determine the magnitude of systematic and random error and their propagation along a levelling line. In order to do this, we check error propagation in our database both using well known methods and analysing original raw height data. The former approach is applied to check the presence of large systematic errors, the latter mainly to quantify random and systematic error propagation.

3.2.1. Slope dependent errors

Large systematic errors are usually slope-dependent, and can be detected by checking the correlation between

elevation and elevation change on the analysed levelling routes. The most important sources of slope-dependent errors are rod calibration and refraction errors (Bomford, 1971). Rod calibration errors are usually detected by using the method proposed by Stein (1981). Following this technique, the elevation change per unit distance (or tilt) is regressed against the gradient of topography. In each of the analysed levelling lines, the correlation of topography with elevation change is not significant, due to the topographic gradient lower than 2%, a value below which the technique is not meaningful (Stein, 1981). Refraction errors largely affect levelling data especially when setup length changes occur between repeated surveys (Holdahl, 1981). In Italy, maximum allowed setup length has not changed from 1950 until now, being of 50 m. Moreover, tests performed on our database (Fig. 3) do not show significant correlations between heights and height changes, which usually indicate the presence of large slope dependent errors (e.g.: Jackson et al., 1981; Reilinger and Brown, 1981; Stein, 1981).

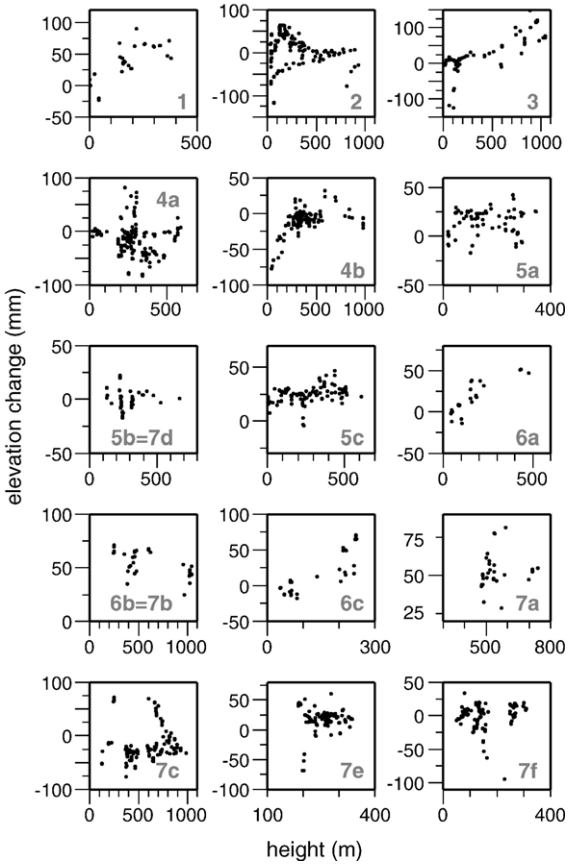

Fig. 3. Heights versus height changes, plotted in order to verify the existence of slope dependent errors. Bottom right numbers indicate transect numbers (letters a to f indicate the levelling lines that compose the transects; lines 5b and 6b are part of transect 7 too). The lack of linear correlation between heights and height changes, allows us to rule out the presence of important rod calibration or refraction errors.

3.2.2. Raw height data analyses

Since raw height data are not easily accessible in the IGM archive, we are forced to use adjusted heights to define vertical movements. However, original raw height data of five sample lines were available in the IGM archive. We collected these data in order to (a) quantify error propagation from forward and backward levelling discrepancies, and (b) verify that the use of adjusted height, instead of raw height data, does not affect elevation change values. We first consider discrepancies between forward and backward levelling of consecutive benchmarks. A series of histogram plots of the 1950 and 2000 discrepancies (Fig. 4a) show that their values are mostly between +2 and −2 mm for each levelling line. In Fig. 4a, the grey bar histograms show that the 2000 values are mostly between 0 and +2 mm. This suggests that there could be some undetected systematic errors that give a greater number of positive values in the 2000 surveys. We use these discrepancies to determine error propagation along the five sample lines. Considering the measurements between consecutive benchmarks (and thus the associated error) as independent, the discrepancies collected for the sample lines can be propagated following a square root law (e.g.: Bomford, 1971). The along line propagation of discrepancies from the arbitrary fixed point (the reference nodal benchmark of each line) is then (Fig. 4b):

$$\text{prop\_err} = \sqrt{\sum_{i=1}^{n} \Delta_i^2},$$

where n is the benchmark number, and Δ_i is the discrepancy value of each measurement between consecutive benchmarks. The measured discrepancies Δ_i (in mm) can be also considered as $\Delta_i \cong \sigma\sqrt{l_i}$, where l_i is the distance (in km) between consecutive benchmarks, σ is the standard error of a 1 km long levelled segment, and $\sigma\sqrt{l_i}$ is the error value between each benchmark pair. Considering a standard deviation of the errors of ±1.0 mm each km of levelled lines, the 1σ well describes the propagation of discrepancies along the sample lines (Fig. 4b). We thus assume that this standard deviation well represents error propagation for the whole dataset, and we use it both for 1950 and 2000 levelling data.

When two different surveys are compared to obtain elevation changes, considering $\sigma_{T1} \approx \sigma_{T2}$ (since the

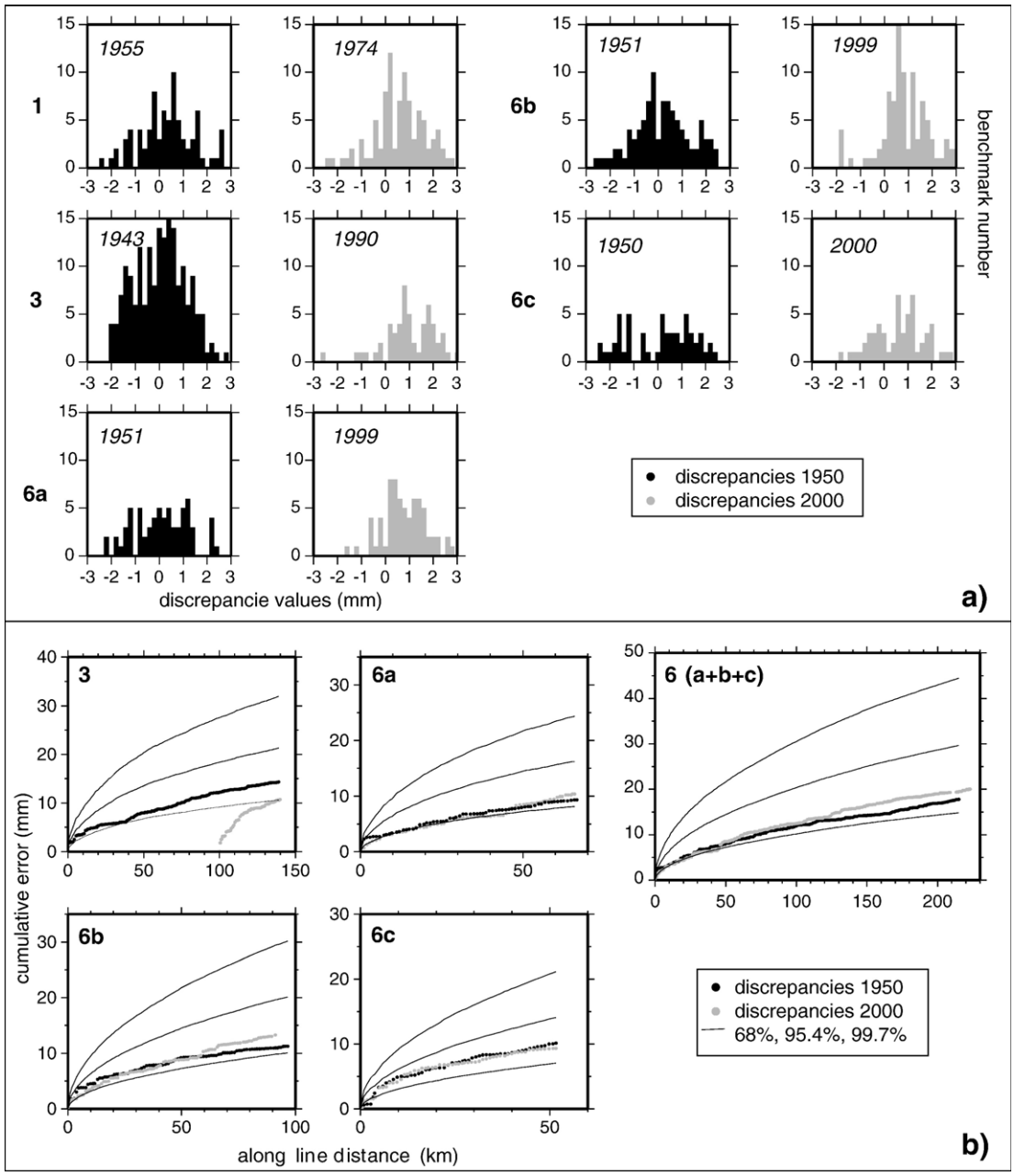

Fig. 4. (a): Histograms showing the values of forward and backward levelling discrepancies for the 1950 (black bars) and 2000 (grey bars) levelling surveys, on the five sample lines; (b): discrepancies propagation along the five sample lines against 1σ, 2σ and 3σ (solid black lines) ($1\sigma = \pm 1$ mm/km$^{1/2}$). Black and grey dots indicate, respectively, 1950 and 2000 values. In figures (a) and (b) bold numbers indicate transect numbers (6a, 6b and 6c indicate the three levelling lines that constitute transect n. 6).

levelling procedures in Italy did not change from 1950 until now), the propagated error is:

$$e_i = \pm\sqrt{2\sum_{i=1}^{n}(\sigma\sqrt{l_i})^2}.$$

It is important to point out that the propagated error e_i indicates the error between the fixed benchmark and the i-th benchmark. This error indicates the maximum allowable random error propagation between the reference and the i-th benchmark along a comparative levelling profile.

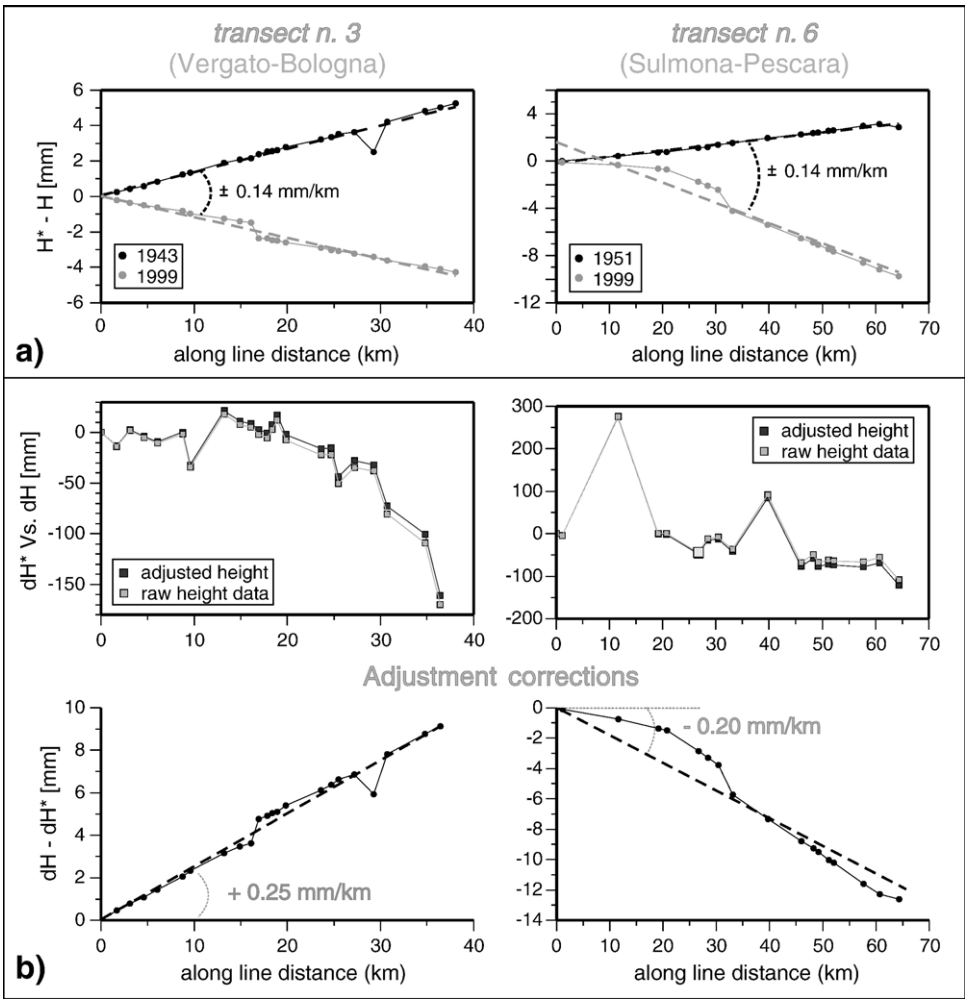

Fig. 5. (a): difference in elevation calculated from adjusted (H) and raw (H*) height data for 1950 (black dots) and 2000 (grey dots) levelling surveys on the last 40 and 65 km of transects 3 and 6, respectively; (b): upper diagrams: elevation changes calculated from adjusted (dH, black squares) and raw (dH*, grey squares) height data for the three sample lines (the second top right diagram represents part of transect 6 made of two levelling lines; nodal benchmark is indicated by the light grey square); lower diagrams: difference between elevation changes calculated from adjusted (dH) and raw (dH*) height data.

Finally, in order to verify if the use of adjusted height instead of raw height data is correct and meaningful for our purposes, we compare elevation and elevation change values resulting from these two datasets. The difference in elevation values given by raw and adjusted heights propagates linearly along the sample lines and grows as ±0.15 mm/km, starting from the reference benchmark (Fig. 5a). When we consider elevation changes occurred between repeated levelling surveys, the difference between raw and adjusted heights rises to about ±0.25 mm/km (Fig. 5b). We consider that both values reflect the corrections applied by IGM during adjustment procedures. The above mentioned values are below the error propagation previously described (Fig. 4b). We thus expect that the calculated error propagation contains all possible differences between raw and adjusted height data. Finally, Fig. 5b (upper diagram) shows that the IGM network adjustment, made to obtain height from measured height differences, does not substantially affect elevation change values.

4. Vertical movements analysis

Using the collected database we assemble 7 traverses (6 nearly perpendicular to the Apennines mountain belt and 1 running along the chain axis) and a vertical velocity field map referred to the tide gauge of Genova (Fig. 2). The main characteristics of each of the 7 transects are

Table 1
Main features of the analysed levelling traverses: (*): number of levelling lines that compose the transect; (**): starting and ending city; profiles in Figs. 6, 8 and 9 are projected from the starting city to the ending one; (***): along line length; (°): years of the "1890," "1950" and "2000" levelling surveys on the 7 traverses; middle and lower rows indicate, respectively, the selected first and second surveys; (°°): maximum relative elevation change within each traverse

Transect no.	No. lev. lines (*)	From − to (**)	Length (***)	Survey years (°)	Max. rel. elev. change (°°)
1	1	Genova–Tortona	75 km	1879 1955 2001	6 cm
2	1	Sarzana–Parma	110 km	1887 1952 2003	12 cm
3	1	Firenze–Bologna	140 km	1889 1943/49 1982/83/85/90	10 cm
4	2	Montepescali–Rimini	270 km	1921 1949/50/51 1989/91	5 cm
5	3	Roma–Fiumesino	280 km	1890 1950/51 1992/97/98/99/2000	4–5 cm
6	3	Taverna Spartimento Pescara	200 km	1893 1950/51 1999/2000	8 cm
7	5	Coste–Firenze	550 km	1950/51 1997/98/99/2000/2001	15 cm

summarized in Table 1. We focus on the "long wavelength" (i.e.: several tens of km) patterns, in order to examine the regional elevation changes during the past 50 years. Regional tectonic movements are determined by the means of polynomial trend lines, which represent the average elevation change pattern of each line, calculated projecting the levelling lines along their mean trajectories (the latter chosen in order to be nearly perpendicular to the chain axis). Four out of the seven traverses are assembled using two or more levelling lines, whereas the map is constructed using all the available 1950 and 2000 measurements. One of the main uncertainties in constructing the assembled traverses and the map is related to the estimation of relative vertical movements occurred at nodal points (i.e.: benchmarks that link two segments levelled in different periods). However, this problem can be considered negligible for each individual traverse, since the time elapsed to measure different segments of the transect is short with respect to the time elapsed between the 1950 and 2000 surveys (see Table 1). Conversely, the construction of the map is more problematic, because the 1950 and 2000 survey periods are variable over the whole network, making the uncertainty on movements occurred at nodal points difficult to be estimated (this issue will be discussed more extensively later in the text).

In the following we first describe the most interesting features of each transect, then we discuss the map. It is important to point out that the resulting elevation changes are to be considered relative values, and do not represent absolute vertical movements.

4.1. Northern Apennines

In northern Apennines, three transects (n. 1, 2 and 3) run nearly perpendicular to the chain (Fig. 6). The observed maximum relative elevation changes are between 6 and 12 cm. Maximum values, for each of the three transects, are located to the N and NE of the drainage divide (Fig. 6a, b and c), towards the external front of the chain (Adriatic side). Transects 2 and 3 show the highest values, that stand significantly above random and systematic error propagation (Fig. 6b and c). These two profiles show an arched upward pattern of elevation changes, with maximum values that occur in proximity of the drainage divide for transect 2 and along the Apennine foothills for transect 3. The regular shape of the three profiles defines signal wavelengths of 30–60 km (Fig. 6d). Looking at the three transects, we note a shift of maximum values toward the Adriatic side of the chain moving from NW to SE. Groundwater withdrawal and/or lithological related subsidence (i.e.: due to unconsolidated Quaternary sediments in the Po Valley) is observed in the north-easternmost sectors of transects 1, 2 and 3 (notice that 2 and 5 benchmarks, showing subsidence exceeding 15 cm, have been removed from

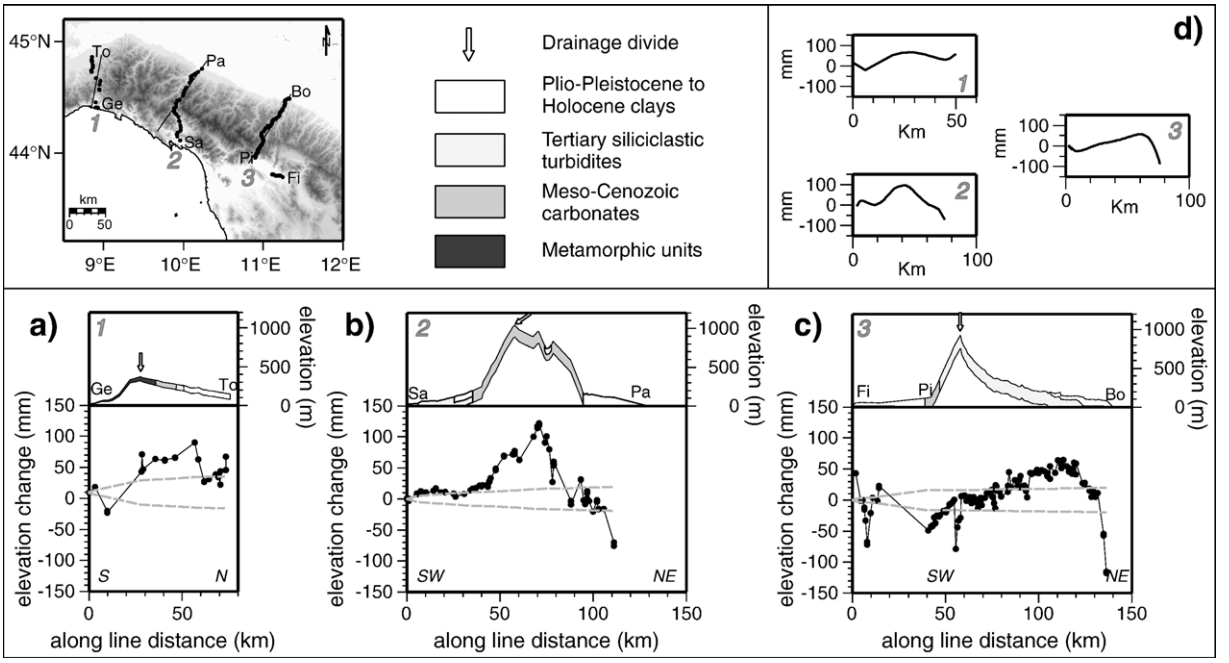

Fig. 6. Northern Apenninic transects. Upper panel shows map (with transect numbers and cities) and legend of the main lithotypes. Lower panel shows: (a) transect n. 1; (b) transect n. 2; (c) transect n. 3. For each transect topography, elevation changes and lithotypes under each benchmark are shown (not to be intended as geological profiles). Dashed lines indicate the allowable accumulation of random error along the lines (i.e.: the propagation of maximum error between benchmarks permitted by IGM). The apparent correlation between elevations and elevation changes in transect n. 2 has been tested with the method of Stein (1981). No significant correlation has been found, and the shown elevation changes are interpreted as due to a tectonic signal. Abbreviations are as follows: Ge = Genova, To = Tortona, Sa = Sarzana, Pa = Parma, Fi = Firenze, Pi = Pistoia, Bo = Bologna (please see also Table 1); (d) envelope of the levelling data projected along the trajectories shown on the map.

profiles of Fig. 6b and c, respectively), as well as in the subsiding Pistoia–Firenze basin of transect 3 (Fig. 6c). An indirect evidence confirming our observations on transects 1, 2 and 3 comes from a transect that runs on the Po Plain, along the Apennines foothills (Fig. 2), crossing large cities like Bologna, Rimini, Forlì and Reggio Emilia, that show subsidence values up to 1.5 m (Fig. 7).

4.2. Central Apennines

In central Apennines two transects (n. 4 and 5) run across the chain in SW–NE and SSW–NNE direction (Fig. 8). The observed profiles show lower elevation change values with respect to the northernmost traverses, with maximum relative differences of 4–5 cm (Fig. 8a

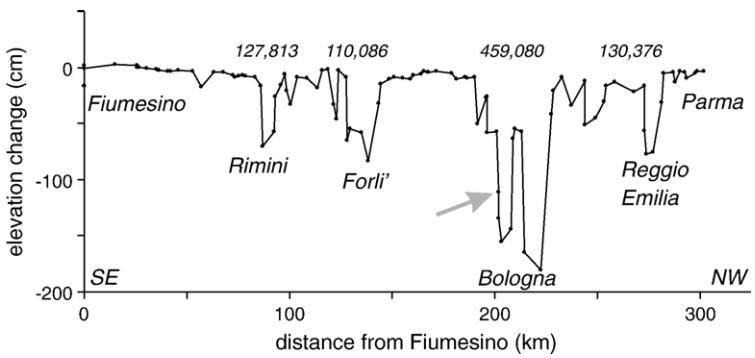

Fig. 7. Elevation changes from the Adriatic coast to the northern Apennine foothills (*via Emilia*), from Fiumesino to Parma (see Fig. 2), measured between 1949–1952 and 1980–1990. The nodal benchmark of Bologna, common to this route and to transect n. 3, is shown by a grey arrow. Population of large cities is also indicated: notice that the highest subsidence corresponds to highest population.

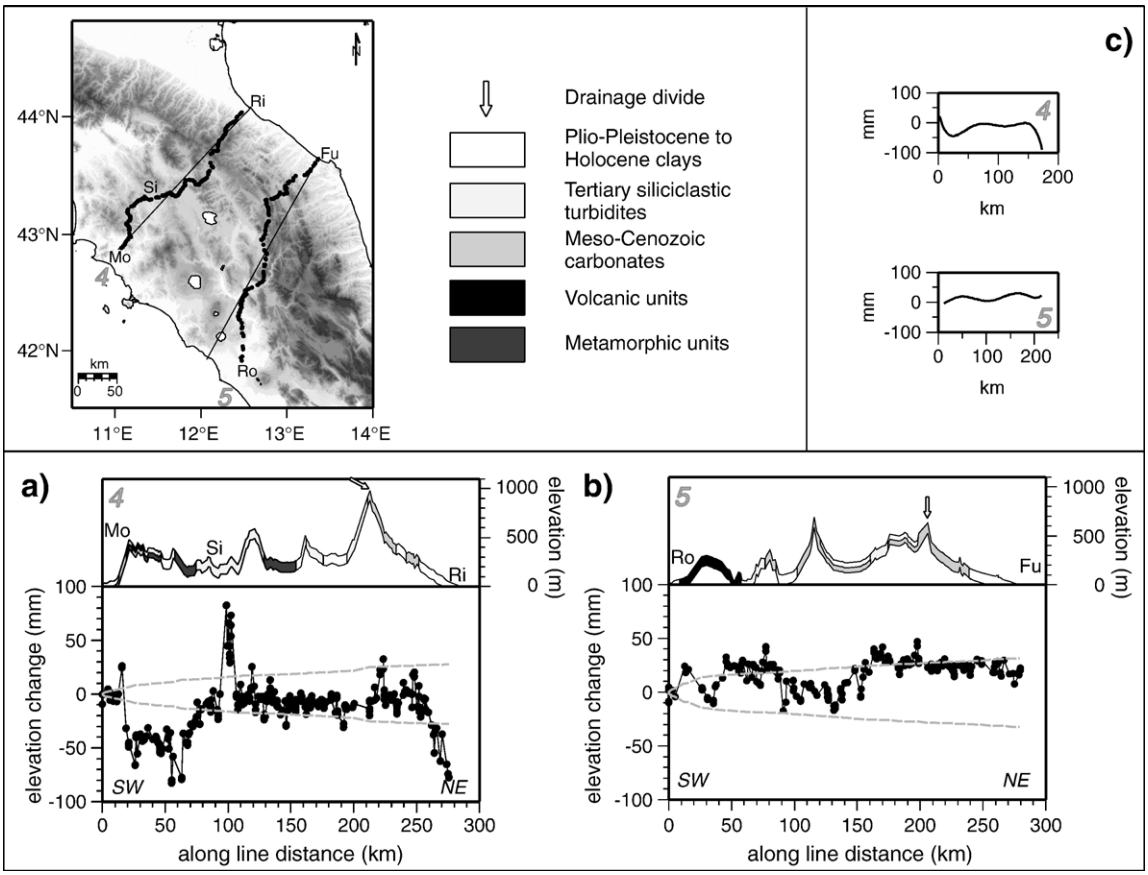

Fig. 8. Central Apenninic transects. Upper panel shows map (with transect number and cities) and legend of the main lithotypes. Lower panel shows: (a) transect n. 4; (b) transect n. 5. For each transect topography, elevation changes and lithotypes under each benchmark are shown (not to be intended as geological profiles). Dashed lines indicate the allowable accumulation of random error along the lines. Abbreviations are as follows: Mo = Montepescali, Si = Siena, Ri = Rimini, Ro = Roma, Fu = Fiumesino (see also Table 1); (c) envelope of the levelling data projected along the trajectories shown on the map.

and b). The shape of elevation change profiles defines wide sectors with similar values of vertical movements (i.e.: no significant movements occur in those sectors), separated by sectors of high gradients of elevation change. The latter are located between km 60 and 90 in transect 4, and km 130 and 160 in transect 5. In transect n. 4 the peculiar elevation change peak shown by 10 benchmarks located around km 100 (near the town of Radicofani, N of Siena), is probably related to the well known geothermal activity of the area (Fig. 8a). In this profile, maximum elevation change values are located at km 170 of Fig. 8a, in a position similar to transect 3. We removed from transect 4 the last 9 benchmarks towards Rimini that show groundwater withdrawal related subsidence (see also Fig. 7). Data from the 1998 survey are excluded from transect 5 (Table 1), because of coseismic displacements related to the 1997 Umbria–Marche earthquake sequence (M_W max = 6.0), previously studied by De Martini et al. (2003). We therefore use the 1992 preseismic measurements. The resulting elevation change profile shows a relatively lowered sector in the internal part of the chain (km 80–150) separated by two rather steep elevation change gradients (Fig. 8b). Summarizing, these two transects differ both for shape and for elevation change magnitude from the northernmost profiles, and maximum values are located in the easternmost sector of transect 4 (Fig. 8a) and on the chain axis in transect 5 (Fig. 8b).

4.3. Central-southern Apennines

Transect n. 6 (Fig. 9a) is the southernmost levelling route running across the Apenninic belt measured in recent time. Maximum observed relative elevation changes, with values up to 8 cm, are located on the higher topographic relief area of this route. The elevation change profile shows a “bulge” shape, with a signal wavelength of 100 km (Fig. 9c). The last 4 benchmarks

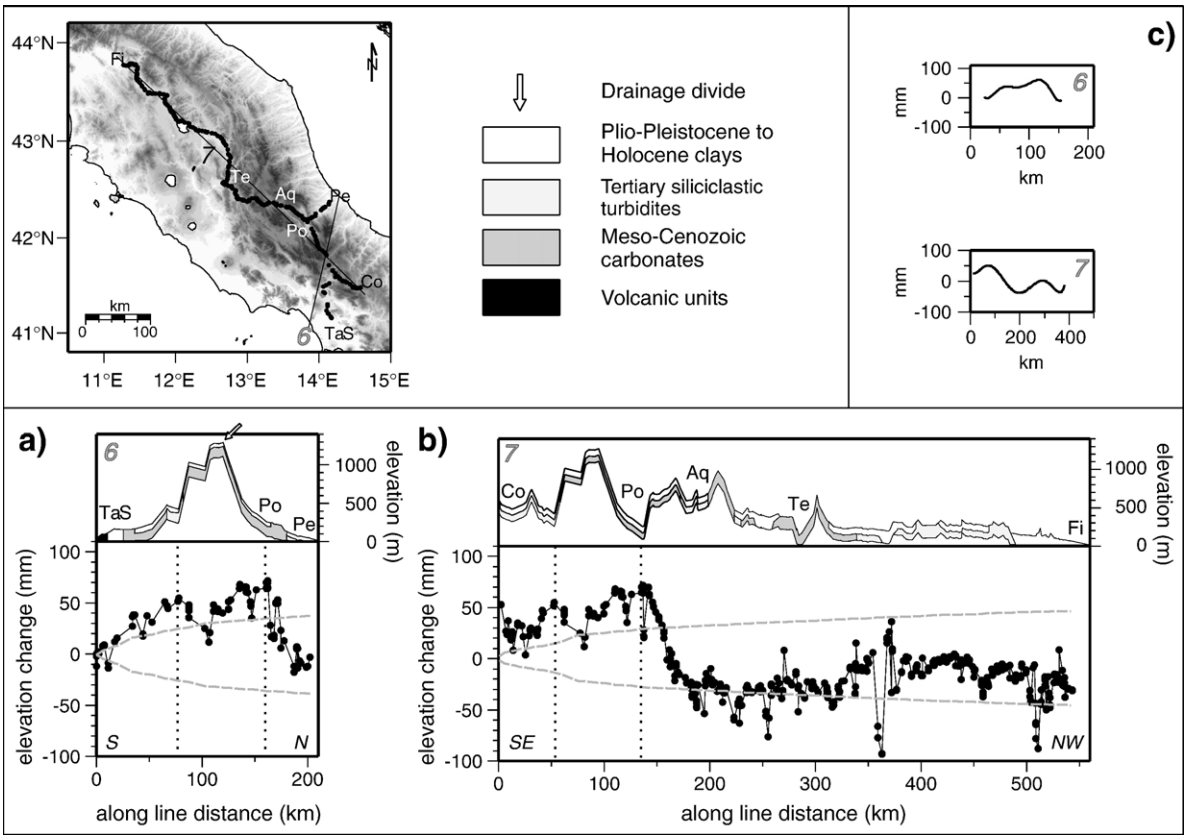

Fig. 9. Southern Apenninic transects. Upper panel shows map (with transect number and cities) and legend of the main lithotypes. Lower panel shows: (a) transect n. 6; (b) transect n. 7. For each transect topography, elevation changes and lithotypes under each benchmark are shown (not to be intended as geological profiles). Dashed lines indicate the allowable accumulation of random error along the lines. Dotted lines indicate the levelling line common to transect n. 6 and 7. Abbreviations are as follows: TaS = Taverna Spartimento, Po = Popoli, Pe = Pescara, Co = Coste, Aq = Aquila, Te = Terni, Fi = Firenze (see also Table 1); (c) envelope of the levelling data projected along the trajectories shown on the map.

toward Pescara showed possible groundwater withdrawal related subsidence up to 30 cm, and have been removed from the profile.

Transect n. 7 (Fig. 9b) runs nearly longitudinal to the Apenninic chain axis. The reference benchmark of this transect is the same of transect n. 6 (Taverna Spartimento), since the two are linked. The most interesting feature of transect 7 is a sharp gradient located between Popoli and L'Aquila, where relative elevation changes show maximum differences of 15 cm, in a 40 km wide sector (Fig. 9b). The remaining sectors of this transect show lower values, with maximum relative differences lower than 4–5 cm (Fig. 9b).

4.4. Summary

Considering the general features of the 7 transects, we notice that: (a) we can exclude the presence of significant random and systematic errors; (b) large part of the elevation changes are above the random and systematic error propagation; (c) line sectors that lie above unconsolidated sediments show a higher signal noise on the observed elevation changes, whereas lines that lie above well consolidated rocks show a less scattered elevation change profile; (d) the observed signal seems to be affected by a "high frequency" noise that shows a maximum amplitude of ± 10–20 mm; (e) the elevation change profiles are not substantially affected by coseismic displacements from earthquakes recorded in the past 50 years, since no significant earthquakes occurred in this time period in proximity of the transects (Boschi et al., 1997; Castello et al., 2004); (f) signal wavelengths are comprised between 30 and 100 km for all the 7 transects, suggesting that these long-wavelengths are related to regional scale tectonic movements.

4.5. Map of current vertical movements

We linked all the collected data together in a unique network, in order to have a relative vertical velocity field

covering the whole Apennines. We calculate all the elevation change rates between 1950 and 2000, using a common reference benchmark. We choose as the arbitrary fixed point the tide gauge of Genova (Fig. 2), because this is the IGM reference benchmark for the peninsular network.

The IGM 1950 and 2000 surveys lasted 15 and 23 years, respectively. When considering repeatedly measured levelling lines, if the time interval between two surveys is relatively large compared to the time used to complete each of them, we can neglect movements occurred during each survey at nodal points (benchmarks that link two different period levelled segments) (Holdahl, 1986). The average time interval between repeated surveys used in this work is 40–50 years, with minimum and maximum values of 26 and 52 years (Fig. 10). Since the time interval between two surveys is short only for a small amount of benchmarks with respect to the whole network (made of 2543 benchmarks) (see Fig. 10), we can assume that movements occurred at nodal benchmarks are negligible.

The resulting vertical velocity field map is shown in Fig. 11. After the removal of 287 benchmarks considered outliers (most of which show subsidence related to human activities) the observed vertical velocities stand in the interval of ±3 mm/a. Most of the levelling lines running along the Adriatic coast show subsidence related to groundwater withdrawal, especially near large cities, with values up to −6 cm/a (not shown on the map) (Fig. 7). Positive vertical velocities are comprised between 0 and 1.5 mm/a, all over the Apennines and on the Tyrrhenian coast (Fig. 11). Two sectors of higher relative elevation changes are located in northern Apennines (transect n. 2) and central-southern Apennines (transects n. 6 and 7),

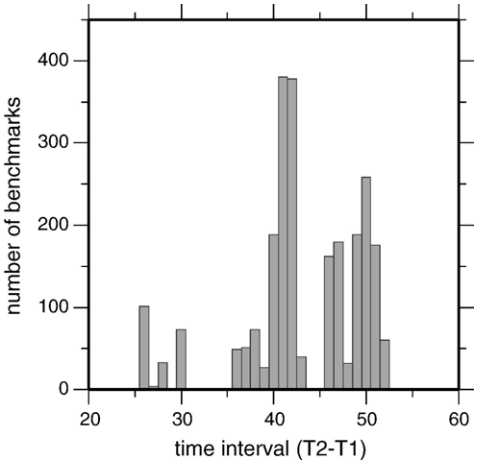

Fig. 10. Time interval elapsed between the 1950 and 2000 levelling surveys for the lines shown in Fig. 11.

the latter being a broad area that span all over the repeatedly measured levelling lines in southern Italy. Unfortunately, the lack of repeatedly measured levelling lines further to the south does not allow us to extend our observations to the whole Apenninic belt.

5. Discussion

We compared our results with those published by Arca and Beretta (1985), which provided a map of vertical movements in northern Apennines for the 1890–1950 time interval, both datasets being referred to the tide gauge of Genova. The comparison is possible only on the three northernmost transects (1 to 3), and show similar uplift shape and similar maximum relative elevation changes for each transect. The main difference is a shift of the absolute elevation change values that increases moving from Genova toward SE. We thus compared our estimates of the 1890–1950 vertical changes on the 6 traverses perpendicular to the Apennines to our results from the 1950–2000 dataset, using an unchanged benchmark of each profile as fixed point (Fig. 12). As the vertical velocity field seems to be nearly constant with time, except for some local movements possibly due to coseismic or groundwater withdrawal related effects, we conclude that these differences can be attributed to the correction and readjustment applied by Arca and Beretta (1985), and to the more scattered data of the 1890–1950 surveys compared to the 1950–2000 ones.

Coseismic movements are observed: in the central part of transects n. 6, in the 1890–1950 dataset, due to the 1915 Avezzano earthquake (M_S=6.7), one of the largest earthquake occurred in central Italy during the last century (CPTI, 1999); in transect n. 2, between 1887 and 1952, possibly related to the 1920 Garfagnana earthquake (M_S=6.5) (CPTI, 1999) (Figs. 11 and 12). On the other hand, transect 4 shows groundwater withdrawal-related movements, occurred between 1950 and 2000, due to the development of the city of Rimini. As a general feature we conclude that shape and magnitude of the vertical velocity field have been almost constant during the last century (note transect 5 of Fig. 12).

A major question can be addressed from the analysis of levelling lines, that is: are the Apennines still growing as they did in the past? The answer would be no, but actually is yes, they are still growing, but not where, and as, expected, and differently along the peninsula.

Geological and geomorphological data related to the uplift of Quaternary repere surfaces exposed along the Apennines suggest a general doming of central-southern Apennines. A post 900 ka regional bulging of southern Apennines is proposed by Cinque et al. (1993), based on

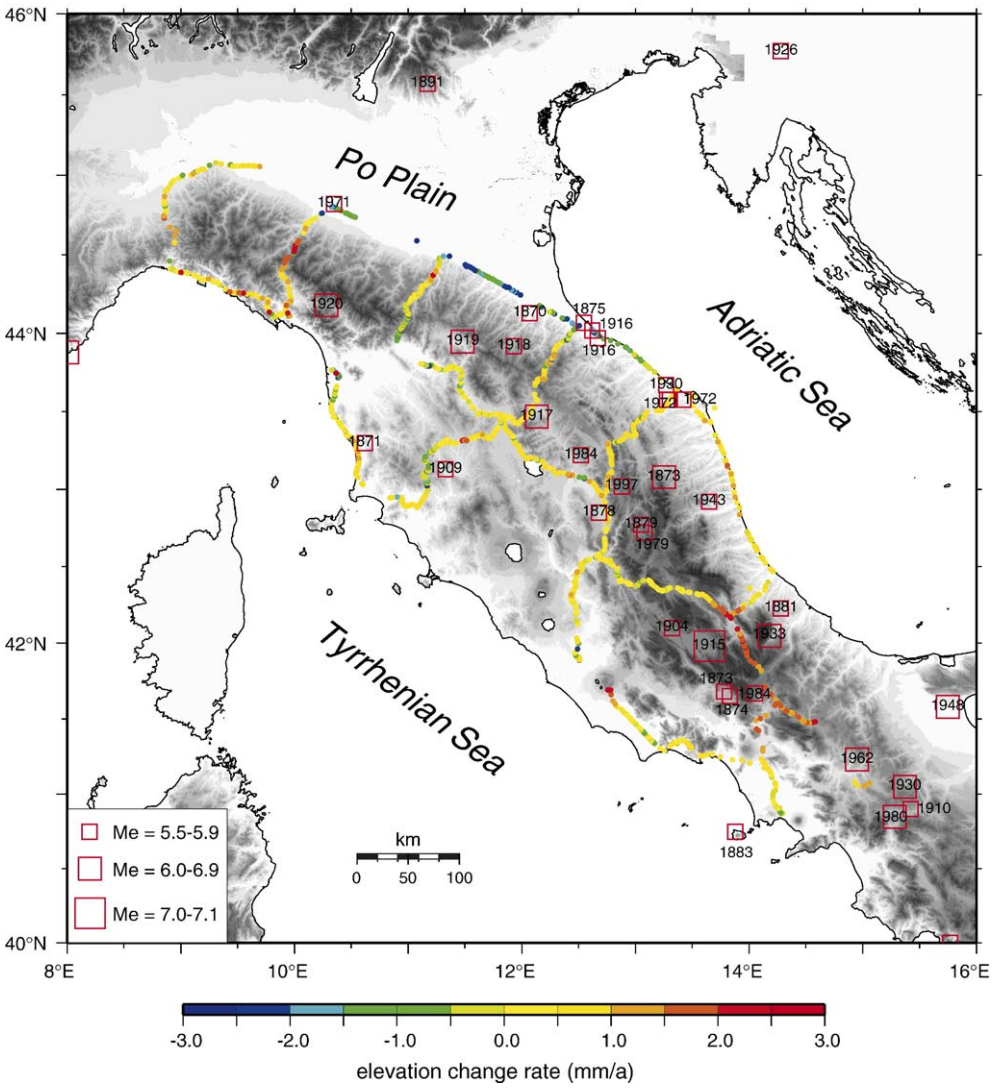

Fig. 11. Elevation change rate map referred to the tide gauge of Genova (see Fig. 1). Earthquakes with $M_e > 5.5$ recorded during the last century are also shown, and the year of occurrence labelled (after Boschi et al., 1997).

the elevation of the *Irsina paleosurface*, a Middle Pleistocene surface that is now exposed at different elevations along the southern Apennines. This bulging is also suggested by Bordoni and Valensise (1998), that, analysing the elevations of marine terraces of the 5e isotopic stage (125 ka) along the Ionian coast, obtain a maximum uplift rate for the Late Pleistocene of 1 mm/a, located in correspondence with the chain axis.

The levelling data herein analysed show that maximum elevation changes are not located where it would be expected. In fact, the shape of relative elevation changes in northern Apennines (transects 1, 2 and 3, Fig. 6) does not coincide with the topographic profile. Rather, maximum values are concentrated east–northeast of the drainage divide and are strongly correlated with the area where active compression is more important, at least from a seismological point of view (Pondrelli et al., 2002; 2004). Although modelling of the calculated signals is out of the scope of the paper, and in progress in a separate paper, the shape of the elevation changes resembles that resulting from interseismic elastic strain accumulation on thrust faults (Jackson and Bilham, 1994). Southeast of the active compressional region, where the extensional tectonics involves greater lengthening rates, the vertical signal is less pronounced (transects 4 and 5, Fig. 8). This could be due to the progressive southeast ending of the compressive tectonics. In fact, from transect 4 down to transect 5 there are not notable elevation changes comparable to the northernmost lines, suggesting that the extensional tectonic

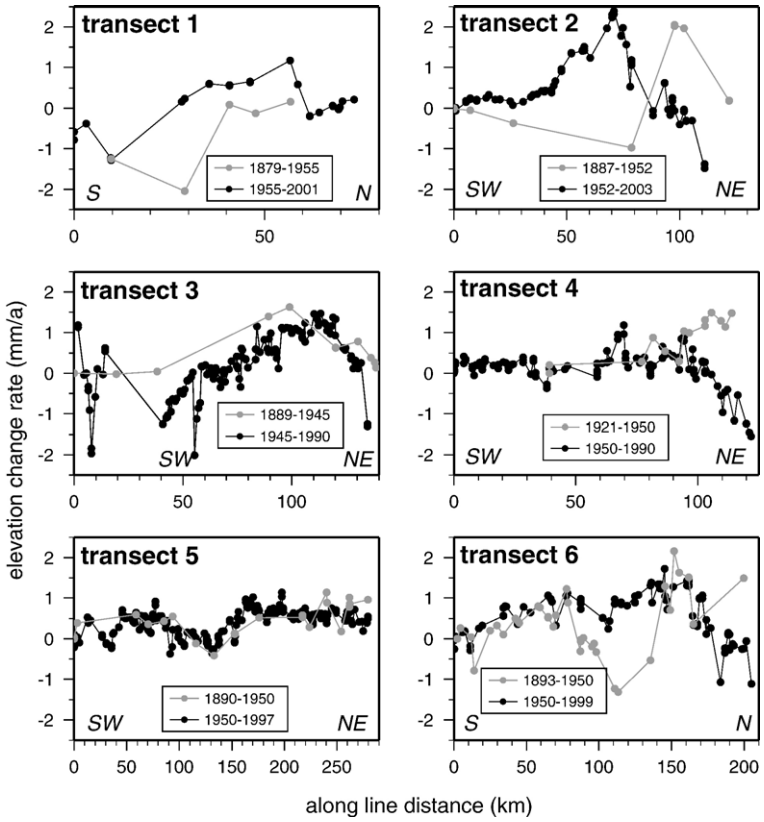

Fig. 12. Elevation change rate profiles for the 1870–1950 and 1950–2000 measurements on the 6 transects running across the Apenninic chain. Survey years are also shown in Table 1.

has not an important signature on vertical motion in central Apennines. Nevertheless, the abrupt positive gradient seen south of L'Aquila (transect 7, Fig. 9) only partly explained by postseismic deformation after the M_W=6.7, 1915, Avezzano earthquake (Amoruso et al., 2005), still remains the main feature of central-southern Apennines. Here, about 2 mm/a of elevation change takes place in few tens of km, and, south of Popoli, the signal is almost flat along the mountain range (transect 7, Fig. 9), decreasing towards the coasts (transect 6, Fig. 9). The lack of more levelling lines crossing the southern Apennines limits the use of these results for a detailed discussion although the bulge-shaped profile seen on transect 6 (Fig. 9) is concentrated in the region of maximum extension rate, differently from what we observe in central-northern Apennines, but similarly to what is observed from geological data in Southern Apennines.

6. Conclusions

On the basis of previously unpublished high precision levelling data we have obtained the vertical velocity field for the past 50 years along and across the northern and central-southern Apennines. The resulting elevation changes are above the random and systematic error propagation. Maximum relative elevation change rates, referred to an arbitrary fixed point (the tide gauge of Genova), are comprised between 1.0 and 3.0 mm/a, and vary along the chain axis. In particular, we can summarize the observations made on the 7 traverses as follows:

1) transects 1 to 3 are characterized by similar shapes and vertical rates. Transects 2 and 3 show an "arched upward" pattern (Fig. 6b and c), with maximum relative rates between 1.5 and 3 mm/a (Fig. 11). Maximum values are located toward the easternmost front of the chain, where focal mechanisms show active compression (Fig. 1);
2) transects 4 and 5 show a nearly homogeneous pattern of vertical rates, with sectors of high gradients (Fig. 8) and maximum relative rates of 1.0–1.5 mm/a (Fig. 11); transect 5 shows a lower sector and zones of positive velocity gradients in correspondence of an area of extensional active tectonic, as indicated by

focal mechanism solutions (Fig. 1) and geodetic data (Hunstad et al., 2003; Serpelloni et al., 2005);

3) transects 6 and 7 (Fig. 9) show maximum relative rates of 2–2.5 mm/a, located on the belt. Southern Apennines experienced the highest seismic strain release during historical times, with the largest earthquake recorded in Italy (Boschi et al., 1997; CPTI, 1999); both transects 6 and 7 (the latter showing a sharp gradient that seems to separate the central and southern Apennines) point out a faster uplift rate of southern Apennines with respect to the central sectors (Fig. 11), although more extended repeated levelling surveys in southern Apennines are required to confirm this feature.

We believe that the data presented in this work contain important information on the accumulation of strain on active faults. Most of the shapes and values shown in Figs. 6, 8 and 9 could be reproduced by elastic or viscoelastic modelling that are out of the scope of the present paper but will be shown in future works.

Acknowledgments

We are grateful to the Istituto Geografico Militare for access to the data, and in particular to M. Bianchi, D. Donatelli, C. Chellini, M. Maglia and P. Giannini for their help during the database collection. We thank N. D'Agostino, C. Chiarabba and A. Amato for helpful discussion. We also thank Christian Sue and an anonymous reviewer for useful comments and criticism. This work is funded by the Civil Protection GNDT project "Probable earthquakes in Italy between year 2000 and 2030: guidelines for determining priorities in seismic risk mitigation." Figures were prepared by using GMT software package (Wessel and Smith, 1995).

Appendix A. Supplementary data

Supplementary data associated with this article can be found, in the online version, at doi:10.1016/j.tecto.2006.02.008.

References

Amato, A., Cinque, A., 1999. Erosional landsurfaces of the Campano–Lucano Apennines (S. Italy): genesis, evolution, and tectonic implications. Tectonophysiscs 315, 251–267.

Amoruso, A., Crescentini, L., D'Anastasio, E., De Martini, P.M., 2005. Clues of postseismic relaxation for the 1915 Fucino earthquake (central Italy) from modeling of leveling data. Geophys. Res. Lett. 32, L22307. doi:10.1029/2005GL024139.

Arca, S., Beretta, G.P., 1985. Prima sintesi geodetico — geologica sui movimenti verticali del suolo nell'Italia Settentrionale (1897–1957). Boll. Geod. Sci. Affini 2, 125–156 (anno XI.IV).

Bartolini, C. 2003. Uplift and erosion: driving processes and resulting landforms. Ed. Quat. Int., 1, 101–102, 280 pp.

Bomford, G., 1971. Geodesy. Oxford University Press, New York. 731 pp.

Bordoni, P., Valensise, G., 1998. Deformation of the 125 ka marine terrace in Italy: tectonic implications. In: Stewart, I.S., Vita-Finzi, C. (Eds.), Coastal TectonicsGeological Society, London, Special Publications, vol. 146, pp. 71–110.

Boschi, E., Guidoboni, E., Ferrari, G., Valensise, G., Gasperini, P., 1997. Catalogue of Strong Italian Earthquake, 461 B.C. to 1990. Istituto Nazionale di Geofisica and S.G.A. (publ.), Bologna 1997, 644 pp. and CD-ROM.

Castello, B., Moro, M., Chiarabba, C., Di Bona, M., Doumaz, F., Selvaggi, G., Amato, A., 2004. Revised magnitudes of relocated Italian earthquakes catalogue (1981–2002): a new seismicity map of Italy. XXII Congress of Gruppo Nazionale di Geofisica della Terra Solida (GNGTS), 14–16 December 2004.

Chiarabba, C., Jovane, L., Di Stefano, R., 2005. A new view of Italian seismicity using 20 years of instrumental recording recordings. Tectonophysics 395, 251–268. doi:10.1016/j.tecto.2004.09.013.

Cinque, A., Patacca, E., Scandone, P., Tozzi, M., 1993. Quaternary kinematic evolution of the Southern Apennines. Relationships between surface geological features and deep lithospheric structures. Ann. Geofis. XXXVI, 249–260.

CPTI Working Group, 1999. Catalogo Parametrico dei Terremoti Italiani. ING, GNDT, SGA, SSN, Bologna, pp. 92 (1999).

D'Agostino, N., Selvaggi, G., 2004. Crustal motion along the Eurasia–Nubia plate boundary in the Calabrian Arc and Sicily and active extension in the Messina Straits from GPS measurements. J. Geophys. Res. 109, B11402. doi:10.1029/2004JB002998.

D'Agostino, N., Jackson, J.A., Dramis, F., Funiciello, R., 2001. Interactions between mantle upwelling, drainage evolution and active normal faulting: an example from the central Apennines (Italy). Geophys. J. Int. 147, 457–497.

De Martini, P.M., Pino, N.A., Valensise, G., Mazza, S., 2003. Geodetic and seismologic evidence for pre and co-seismic slip along a low-angle, blind normal fault, and implications for active faulting studies. Geoph. J. Int. 55 (3), 819–829 (December).

Holdahl, S.R., 1981. A model of temperature stratification for correction of levelling refraction. Bull. Geod. 55, 231–249.

Holdahl, S.R., 1986. Readjustment of levelling networks to account for vertical coseismic motions. Tectonophysics 130, 195–212.

Hunstad, I., Selvaggi, G., D'Agostino, N., England, P., Clarke, P., Pierozzi, M., 2003. Geodetic strain in peninsular Italy between 1875 and 2001. Geophys. Res. Lett. 30 (4), 1181. doi:10.1029/2002GL016447.

Jackson, M., Bilham, R., 1994. Constraints on Himalayan deformation inferred from vertical velocity fields in Nepal and Tibet. J. Geophys. Res. 99 (B7), 13,897–13,912.

Jackson, D.D., Lee, W.B., Liu, C., 1981. Height dependent errors in Southern California levelling. In: Simpson, David W., Richards, P.G. (Eds.), Maurice Ewing series 4, Earthquake Prediction — An International Review. American Geophysical Union, pp. 457–472.

Muller, G., 1986. Appunti di Livellazione. Collezione dei Testi Didattici dell'Istituto Geografico Militare. 92 pp.

Patacca, E., Scandone, P., 2001. Late thrust propagation and sedimentary response in the thrust–belt–foredeep system of the Southern Apennines (Pliocene–Pleistocene). In: Vai, G.B., Martini, I.P. (Eds.), Anatomy of an orogen: the Apennines and

adjacent Mediterranean basins. Kluwer Academic Publishers, pp. 401–440.

Pondrelli, S., Morelli, A., Ekström, G., Mazza, S., Boschi, E., Dziewonski, A.M., 2002. European–Mediterranean regional centroid moment tensors: 1997–2000. Phys. Earth Planet. Inter. 130, 71–101.

Pondrelli, S., Morelli, A., Ekstrom, G., 2004. European–Mediterranean Regional Centroid Moment Tensor catalog: solutions for years 2001 and 2002. Phys. Earth Planet. Inter. 145, 127–147. doi:10.1016/j.pepi.2004.03.008.

Reilinger, R., Brown, L., 1981. Neotectonic deformation, near-surface movements and systematic errors in U.S. relevelling measurements: implications for earthquake prediction. In: Simpson, D.W., Richards, P.G. (Eds.), Earthquake Prediction: An International Review, Maurice Ewing Ser., vol. 4, pp. 422–440. AGU.

Salvioni, G., 1951. Manuale di Livellazione. Collezione dei Testi Tecnici dell'Istituto Geografico Militare, Firenze. .

Salvioni, G., 1953. Primo contributo sulla comparazione dei risultati fra la nuova rete altimetrica fondamentale e la vecchia livellazione di precisione. Boll. Geod. Sci. Affini XII (I), 87–97.

Salvioni, G., 1957. I movimenti del suolo nell'Italia centro-settentrionale, dati preliminari dedotti dalla comparazione di livellazioni. Boll. Geod. Sci. Affini XVI (3), 325–366.

Serpelloni, E., Anzidei, M., Baldi, P., Casula, G., Galvani, A., 2005. Crustal velocity and strain-rate fields in Italy and surrounding regions: new results from the analysis of permanent and non-permanent GPS networks. Geophys. J. Int. 161, 861–880. doi:10.1111/j.1365-246X.2005.02618.x.

Stein, R., 1981. Discrimination of tectonic displacement from slope dependent errors in geodetic levelling from Southern California, 1953–1979. In: Simpson, David W., Richards, P.G. (Eds.), Maurice Ewing series 4, Earthquake prediction, An International Review. American Geophysical Union, pp. 441–456.

Vignal, J., 1936. Evaluation de la precision d'une methode de nivellement. Bull. Geod. 49, 1–159.

Vignal, J., 1950. Comptes rendus des séances de travail de la Secion II. Nivellments, de l'Assocation Internationale de Géodésie à l'Assemblée Générale d'Oslo (Aout 1948). Bull. Géod. 18, 401–565.

Wessel, P., Smith, W.H.F., 1995. New version of the Generic Mapping Tools released. Eos Trans. AGU 76 (33), 329.